Crossing barriers, delivery of llama antibody fragments into the brain

Rotman, M.

4

CHAPTER

FUSION OF HUMAN FC TO VHH-PA2H INCREASES BLOOD RESIDENTIAL TIME, BUT NOT BRAIN UPTAKE

Adapted from

Fusion of hIgG1-Fc to ^{111}In-anti-amyloid single domain antibody fragment VHH-pa2H prolongs blood residential time in APP/PS1 mice but does not increase brain uptake.

Maarten Rotman [1,2], Mick M. Welling [2], Marlinde L. van den Boogaard [1], Laure Grand Moursel [1,2], Linda M. van der Graaf [1,2], Mark A. van Buchem [2], Silvère M. van der Maarel [2] and Louise van der Weerd [2,3].
Nuclear Medicine and Biology **42** (2015) 695-702

ABSTRACT

Introduction: Llama single domain antibody fragments (VHH), which can pass endothelial barriers, are being investigated for targeting amyloid plaque load in Alzheimer's disease (AD). Contrary to conventional human or murine antibodies consisting of IgG or F(ab')2 antibody fragments, VHH are able to effectively pass the blood-brain barrier (BBB) *in vitro*. However, in earlier *in vivo* studies, anti-amyloid VHH showed poor BBB passage due to their short serum half-lives. It would be of interest to develop a VHH based protein with elongated serum half-life to enhance BBB passage, allowing the VHH to more easily reach the cerebral amyloid deposits.

Methods: To increase serum persistence, the Fc portion of the human IgG1 antibody (hinge plus CH_2 and CH_3 domains) was fused to the C-terminus of the VHH (VHH-pa2H-Fc). To determine the pharmacokinetics and biodistribution profile of the fusion protein, the chelator p-SCN-Bz-DTPA was linked to the protein and thereafter labelled with radioactive indium-111 (^{111}In). Double transgenic APP_{swe}/PS1dE9 and wildtype littermates were injected with 20 µg VHH-pa2H-Fc-DTPA-^{111}In (10-20 MBq). Pharmacokinetics of the tracer was determined in blood samples at 10 intervals after injection and imaging using microSPECT was performed. The biodistribution of the radioactivity in various excised tissues was measured at 48 h after injection.

Results: We succeeded in the expression of the fusion protein VHH-pa2H-Fc in HEK293T cells with a yield of 50 mg/ml growth medium. The fusion protein showed homodimerization – necessary for successful Fc neonatal receptor recycling. Compared to VHH-pa2H, the Fc tailed protein retained high affinity for amyloid beta on human AD patient brain tissue sections, and significantly improved serum retention of the VHH. However, at 48 h after systemic injection of the non-fused VHH-pa2H-DTPA-^{111}In and the VHH-pa2H-Fc-DTPA-^{111}In fusion protein in transgenic mice, the specific brain uptake of VHH-pa2H-Fc-DTPA-^{111}In was not improved compared to non-fused VHH-pa2H-DTPA-^{111}In.

Conclusion: Using VHH-Fc conjugates increases the blood half-life of the protein. However, purely extending the time window for brain uptake does not increase BBB passage. Nevertheless, VHH-Fc holds promise for therapeutic applications where a sustained systemic circulation of VHH is advantageous.

1. INTRODUCTION

Due to their long, protruding and highly variable CDR3 section, llama derived single domain antibody fragments (VHH) have the ability to access epitopes normally hidden for conventional antibodies. As such they are a very successful class of therapeutics, with applications ranging from interference with enzymatic active sites leading to neutralization of toxins [1–3] and viruses [4], blocking of apoptotic pathways in autoimmune diseases [5] and preventing aberrant protein aggregations [6], to binding spatially different amyloid beta (Aβ) depositions [7].

On the other hand, their small size (12-15 kDa) and inherent short blood half-life can be a hindrance to target their epitopes. Monovalent VHH may not have enough time to interact with hard-to-reach epitopes or to cross regulated endothelial barriers – such as the blood-brain barrier (BBB) – in sufficient amounts [8]. They may be rapidly filtered out of the system, unless they are either injected at very high doses, or continuously via infusion or unless the BBB is locally impaired [9,10]. Even though for imaging applications short half-lives are interesting [11], for systemic immunotherapeutic applications, elongated serum half-lives of VHH are preferred. For our application of VHH as amyloid targeting therapeutics, both increased BBB passage and extension of serum half-life would be desired and the second may prove to be a means to achieve the first.

Elongation of serum half-life time of unmodified VHH can be achieved by repeated injections or slow infusion administration [12,13], but a less invasive, and thus preferable way to increase serum retention is by fusing the antibody fragment to an IgG fragment crystallizable region (Fc, i.e. CH_2 and CH_3) and the hinge region. Due to the inherent dimeric nature of the Fc fragment, VHH-Fc fusions are produced as homodimeric proteins with interchain disulfide bridges between the cysteine amino acids in the hinge region [14]. The total protein complex size of the dimeric VHH-Fc increases to 80 kDa, i.e. above the molecular weight cut-off limit of globular filtration by the kidneys, which is approximately 60 kDa. Additionally, the CH_2 and Ch_3 domains will interact with the neonatal Fc receptor (FcRn) in early endosomes, favoring recycling and transcytosis over catabolism, which in turn increases the retention of the protein in the body [15–17].

The Fc-fusion approach has been performed earlier with single chain antibody fragments (scFv) [12,13], which too are recombinant antibody fragments. These scFv-Fc fusion proteins have been produced and applied both *in vitro* and *in vivo* [18–20], and studies indeed show increased blood residential times of the constructs [21]. VHH-Fc fusion constructs have been developed and produced in plant cells [22–24] as well as in cultured murine cell lines [2] as in cultured human cell lines [5,25]. However, until very recently the *in vivo* biodistribution profiles of VHH-Fc fusion proteins have not been extensively reported, with a single reference reporting a

generally increased blood half-life in BALB/c mice [26] and one more extensive report showing improved pharmacokinetic potency and increased BBB passage in Wistar rats [27].

This study reports on the production and validation of an Fc-fusion VHH directed against human Aβ and the pharmacokinetics and biodistribution profiles of this Fc-fusion VHH in transgenic APPswe/PS1dE9 mice compared to the unmodified VHH antibody fragment. Here we describe the production in human embryonic kidney cells (HEK293T) and purification of anti-Aβ VHH-pa2H fused to the Fc domain and hinge region of a human IgG1. Furthermore, we determined whether specific affinity for Aβ in pathological brain materials was retained for the secreted fusion protein. Finally, we measured and describe the biodistribution profile and performed SPECT imaging in mice using the radiolabeled VHH-Fc to show the effect of increased retention in the blood on BBB passage.

2. MATERIALS AND METHODS

2.1. Construction of VHH-pa2H-Fc in pINFUSE-hIgG1-Fc1 vector

VHH-pa2H was cloned from the pUR5071 vector [7] into an intermediate subcloning vector to introduce the chicken lysozyme secretion signal (ss)) [5'-ATGAGGTCTTTGCTAATCTTGGTGCTTTGCTTCCTGCCCCTGGCTGCTCTGGGG-3'] [28] directly upstream of the VHH (SS-VHH-pa2H). A BglII and an EcoRI restriction enzyme consensus sequence were introduced respectively upstream and downstream of the ss-VHH-pa2H sequence via PCR [fwd primer BglII: 5'-agaagatctcgcagcagctgaggat-3'; rev primer EcoRI: 5'-gcagaattcatgaggtctttgctaatctt-3']. The construct was then cloned into a pINFUSE-hIgG1-Fc1 vector (InvivoGEN, USA) using the introduced restriction sites, to create the ss-VHH-pa2H-hIgG1-Fc (VHH-pa2H-Fc) fusion protein construct under the control of a hEF1-HTLV composite promotor (Figure 4.1).

2.2. Production of VHH-pa2H-Fc in HEK293T and quality control

The VHH-pa2H-Fc fusion protein was produced in HEK293T cells under serum-free conditions as described before [29]. The fusion protein contained in the cell-free medium fraction was affinity purified using Protein A resin (nProteinA sepharose 4 Fast Flow, GE Healthcare, NL). After washing with PBS, the VHH-pa2H-Fc was eluted from the Protein A resin with 0.1 M sodium citrate at pH 2.0. Fractions containing the purified VHH-pa2H-Fc were pooled and neutralized to pH 7.5 by adding 1M NaOH buffer solution and dialyzed three times against PBS including one step overnight. The amount of purified protein was assessed using the Bradford assay and Nanodrop® spectral absorption at 280 nm. The purity of VHH-pa2H-Fc was determined with size exclusion chromatography on an ÄKTA FLPC system (GE Healthcare) using a size

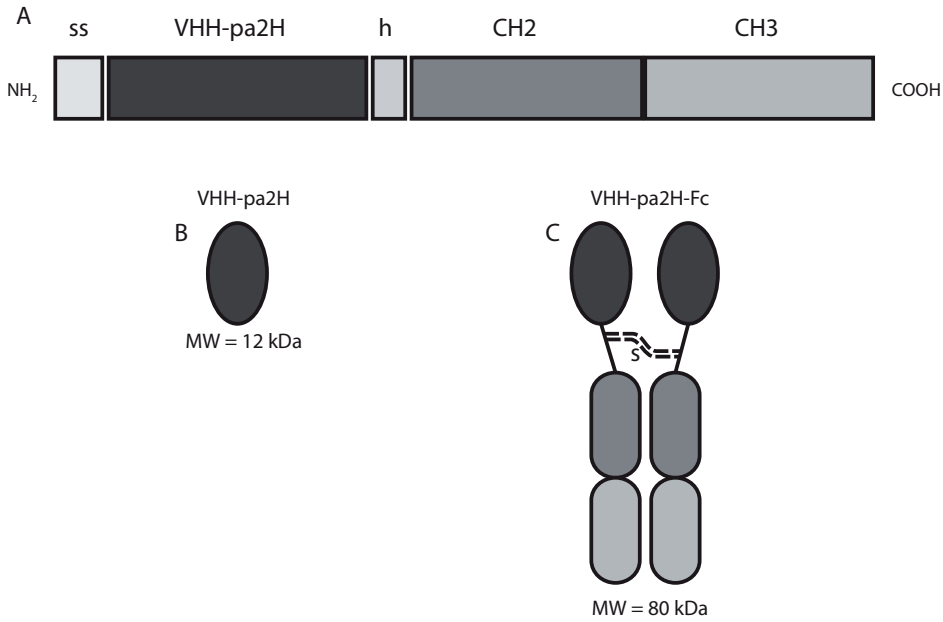

Figure 4.1. Schematic representation of ss-VHH-pa2H-Fc. **(A)** The llama antibody fragment pa2H is fused to the hinge (h) region and the CH_2 and CH_3 domains of the crystallizable fragment (Fc) of the human IgG1. The N-terminal lysozyme secretion signal (ss; amino acid sequence MRSLLILVLCFPLAAGAQPA) forces the protein to be secreted into the extracellular space. **(B + C)** Due to the fusion of the Fc domain, the VHH-pa2H, which is normally 12 kDa in size, will form two disulfide bridges in the attached hinge region and reach a total size of approximately 80 kDa as a homodimeric protein complex.

exclusion column (SuperdexTM 75 10/300 GL). To confirm the formation of the homodimeric VHH-pa2H-Fc products, purified samples were on SDS-PAGE under reducing and non-reducing conditions. Reduced VHH-pa2H-Fc samples were prepared with dithiothreitol (DTT; Sigma, NL), whereas in the non-reducing conditions DTT was omitted. Purified VHH-pa2H-Fc was stored at 4°C until use. For comparison studies non-fused VHH-pa2H was produced as described before [8].

2.3. Immunofluorescence analysis

To confirm the retained affinity of VHH-pa2H-Fc and VHH-pa2H-Fc-DTPA (see section 2.4.) for Aβ depositions, immunofluorescence staining was performed on human post-mortem AD brain and aged matched healthy control cryosections. All human tissues were obtained from anonymous patients or healthy aged donors as confirmed by neuropathological examination in agreement with the guidelines of the Medical Ethics Committee of the Leiden University Medical Center, The Netherlands. All tissues were processed in a coded fashion, according to Dutch national ethical guidelines (Code for Proper Secondary Use of Human Tissue, Dutch Federation of Medical Scientific Societies). Briefly, acetone fixed serial cryosections (5 μm) were blocked for 1-2 h with 4% milk powder (Marvel dried skimmed milk powder, Premier

Foods, UK) in PBS (mPBS). Blocked sections were incubated overnight with 20 ng/µl purified VHH-pa2H-Fc or VHH-pa2H-Fc-DTPA. After 3 × 5 min. washing steps with PBS, the sections were exposed to mouse anti human IgG1 (1:500, m1325 Sanquin Peliclass, NL) for 1-2 h, washed and then incubated with Alexa Fluor 488 – goat anti mouse (1:500, A-11001, Life Technologies, USA) for 1 h. To confirm Aβ presence, adjacent mPBS blocked sections were incubated with mouse anti Aβ (4G8, Covance, NL) for 1 h, washed and then incubated with Alexa Fluor 594 – goat anti mouse (1:500, A-11032, Life Technologies) for 1 h. All antibody dilutions were performed in mPBS. Fluorescence signal was detected on a Leica DM5500B microscope with a Leica DFC360FX camera and analyzed with Leica LAS-AF v.2.3.6 software (Leica Microsystems, NL). Whole slide overview images were acquired with a BZ-9000 BIOREVO HS All-in-One Fluorescence microscope (Keyence, BE).

2.4. DTPA conjugation to VHH-pa2H-Fc and radiolabeling with indium-111

To enable the radiolabeling of the VHH with indium-111 (^{111}In), the chelator p-SCN-Bn-DTPA ($C_{22}H_{28}N_4O_{10}S{\cdot}3HCl$, MW 649.92 g/mol, Macrocyclics Inc., USA) was conjugated to primary amine groups on the VHH-pa2H-Fc fusion protein as described previously [8]. In short, a 5 × molar excess of the chelator was incubated with VHH-pa2H-Fc at 37°C for 3 h in PBS at pH 8.2 and dialyzed against the labeling buffer 250 mM ammonium acetate at pH 5.5 for at three times at 4°C including one overnight step. Conjugated and dialyzed preparations were stored in the dark at 4°C.

Before *in vivo* use, the VHH-pa2H-Fc-DTPA construct was radiolabeled with ^{111}In though incorporation of the isotope into the DTPA chelator as described before [8]. In short $^{111}InCl_3$ (Covidien, NL) was added to the DTPA conjugated VHH-Fc, incubated at 37°C in 250 mM ammonium acetate buffer at pH 5.5 for 3 h under gentle shaking, and then purified with a PD-10 desalting column (GE Healthcare) in 20 elution fractions of 0.5 ml PBS. Fractions containing radioactive ^{111}In-labeled VHH-pa2H-Fc-DTPA (VHH-pa2H-Fc-DTPA-^{111}In) were pooled and used for animal studies. The amount of $^{111}InCl_3$ added to the labeling solution was adjusted depending on radiation strength upon delivery to yield 20 µg of VHH-pa2H-Fc-DTPA-^{111}In at 10-20 MBq per injection.

2.5. Pharmacokinetics

All *in vivo* studies were performed using 12-16 month old double transgenic mice (n = 4-8) from a colony set up using the APPswe/PS1dE9 strain (APP/PS1; JAX® Mice and Services, The Jackson Laboratory, USA) on a C57BL/6 background and their wildtype littermates (WT). The strain is known to rapidly develop a vascular (CAA) and parenchymal Aβ associated phenotype [30–32]. Animals were kept on a strict 12 h day/night light cycle with unlimited access to nor-

mal chow and water. All animal studies have been approved by the Leiden University Medical Center institutional Animal Experiments Committee (DEC permits 10097 and 12065). Besides standard genotyping, Aβ pathology was confirmed on brain sections by standard Thioflavin T staining [10].

Animals were injected intravenously with 20 μg VHH-pa2H-Fc-DTPA-^{111}In (10-20 MBq). At 0.5, 2, 3, 4, 6, 22, 24, 26, 28 and approximately 48 h after injection 5 μl blood samples were taken from the tail vein and counted for radioactivity. After correction for radioactive decay, the total injected dose (ID), blood clearance rates, area under the curve values (AUC) and standard uptake values (SUV, i.e. the percentage of the ID per gram blood – or gram tissue – per gram mouse) in blood were calculated as described before [8].

2.6. MicroSPECT imaging

To visually analyze the biodistribution profiles, transgenic and WT animals, injected with the radiolabeled VHH-pa2H-Fc-DTPA-^{111}In, were imaged for 40 minutes under continues 1-2% isoflurane inhalation anesthesia on a three-headed U-SPECT-II microSPECT (MILabs, NL). Images were obtained at 48 h after administration of the radiolabeled VHH using a 0.6 mm mouse pinhole collimator, and energy setting at 171 keV with a window of 20% [8]. Total body images were reconstructed using six POSEM iterations with 16 subsets, a 0.2 mm voxel size and with decay and scatter corrections integrated into the reconstruction using dedicated MILabs reconstruction software. Volume-rendered images were generated and analyzed using a freeware tool from Amide.exe 1.0.2 Medical Image Data Examiner (http:/amide.sourceforge.net) [8,33].

2.7. Biodistribution

Directly after imaging and collecting the last blood sample, the mice were euthanized and perfused with 15 ml PBS [8]. Thereafter, the bladder including urine, heart, lungs, spleen, liver, both kidneys, part of the left femoral muscle, cerebrum, and cerebellum were removed. All tissues and organs were weighted and counted for radioactivity using a Wizard2 2470 automatic gamma scintillation counter (Perkin Elmer, USA) and obtained measurements of radioactivity uptake in tissues and organs were calculated and reported as SUV.

2.8. Statistical analysis

All data are presented as mean value (±SEM) of 4-8 independent measurements. Statistical analysis for differences between groups in the animal studies were performed by Student's paired t-test with one-tailed distribution. Significance was assigned for p-values of <0.05. All analyses and calculations were performed using Microsoft® Office Excel 2010 and GraphPad Prism version 5.01 for Windows (GraphPad Software, USA).

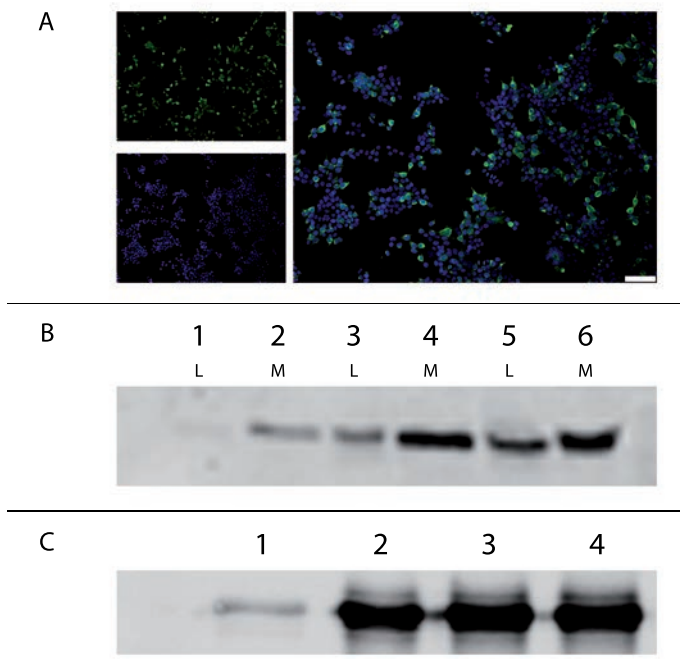

Figure 4.2. HEK293T production of VHH-pa2H-Fc. **(A)** Transfection of HEK293T cells with the pINFUSE-ss-VHH-pa2H-Fc vector and PEI transfection reagent consistently yields high transfection efficiencies. Blue channel shows DAPI stained nuclei, green channel shows VHH-pa2H-Fc stained with mouse-anti-hIgG1 and Alexa Fluor – 488 goat-anti-mouse. White bar indicates 75 μm. **(B)** Western blot analysis of the effect of Fetal Calf Serum (FCS) in the medium indicates the need for FCS during the first 24 h after transfection. Lanes 1 and 2 = 0% FCS, lanes 3 and 4 = 10% FCS during the first 24 h, 0% FCS during the second 24 h, lanes 5 and 6 = 10% FCS. Samples were taken 48 h after transfection. L = cell lysate sample, M = cell-free medium sample. Bands run at approximately 42 kDa. Primary antibody: mouse-anti-hIgG1, secondary antibody: IRD-CW800-goat-anti-mouse. **(C)** VHH-pa2H-Fc secreted into the cell medium at 0, 24, 48 and 72 h after switching to FCS free medium at 24 h after transfection (lanes 1 to 4, respectively) indicate immediate and effective secretion of the produced VHH-pa2H-Fc fusion protein. Bands run at approximately 42 kDa. Primary antibody: mouse-anti-hIgG1, secondary antibody: IRD-CW800-goat-anti-mouse.

3. RESULTS

3.1. VHH-pa2H-Fc production and quality control

Transfection of pINFUSE-ss-pa2H-Fc into HEK293T cells yielded high transfection efficiencies (Figure 4.2 A) and nearly immediate production and secretion of the fusion protein (Figure 4.2 B and C). The best production and purification of VHH-pa2H-Fc was obtained with transfection in medium supplemented with fetal calf serum (FCS) and maintained in FCS-free condition from 24 h after transfection. This set-up yielded 50 mg secreted VHH-pa2H-Fc per litre growth medium, at an average final concentration after purification and dialysis of 1.0 mg/ml VHH-pa2H-Fc in PBS.

The produced and secreted VHH-pa2H-Fc and the VHH-pa2H-Fc-DTPA both retained functional specificity for Aβ depositions in plaques and around vessel walls in brain tissue sections from

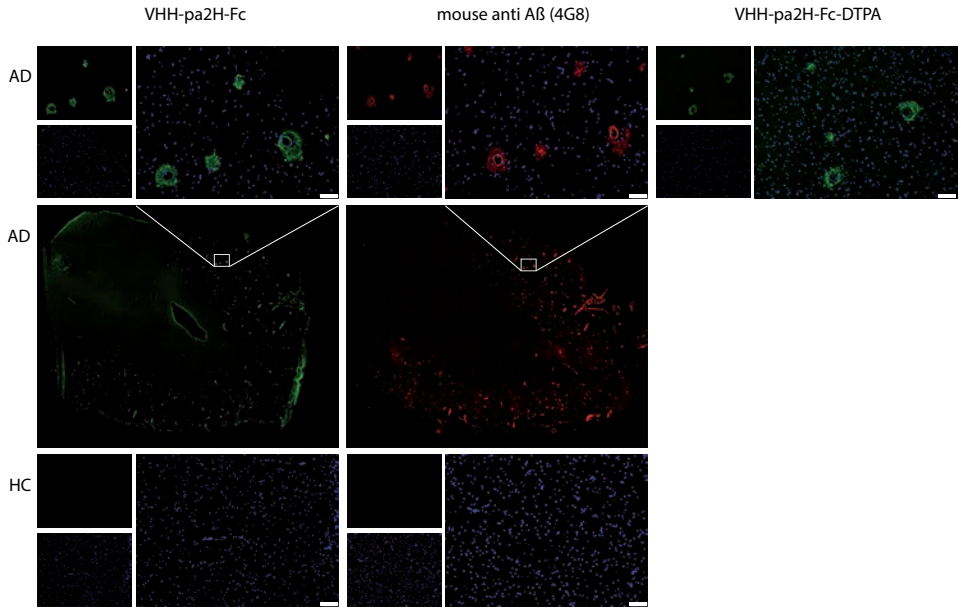

Figure 4.3. IHC on serial sections of *post mortem* patient brain material (AD) and aged matched healthy control (HC) stained for amyloid deposits with either VHH-pa2H-Fc (left: green) or VHH-pa2H-Fc-DTPA (right: green) or 4G8 (middle: red) show outstanding and highly specific recognition of VHH-pa2H-Fc for both vascular and parenchymal Aβ, regardless of DTPA conjugation. Secondary antibody: mouse-anti-human IgG for the VHH; Alexa Fluor 594 – goat-anti-mouse for the 4G8 staining. Tertiary antibody for the VHH-pa2H-Fc and VHH-pa2H-Fc-DTPA only: Alexa Fluor 488 – goat-anti-mouse. Nuclei stained in blue with DAPI. Top row images represent vascular and parenchymal amyloid deposits, middle row shows the remainder of the section and bottom row images are representative of parenchymal and vascular areas in aged matched healthy controls devoid of Aβ deposits. White bars indicate 75 μm.

human patient material and does not show a specific binding in control tissue (Figure 4.3). The immunoreactivity is highly similar to conventional monoclonal anti-Aβ antibodies (e.g. clone 4G8) and to the specificity previously shown by unmodified VHH-pa2H [7,8,10,30]. Addition of the chelator DTPA to VHH-pa2H-Fc did not impair the ability to recognize and bind Aβ.

3.2. VHH-pa2H-Fc dimerization

For interaction of the VHH-Fc with FcRn, which is necessary to prolong the blood half-life, the fusion protein must form disulphide bridge based dimers as shown in Figure 4.1. The formation of the homodimers was confirmed on SDS-PAGE under reducing and non-reducing conditions. Under reducing conditions the VHH-Fc fusion protein ran at the expected monomer height of approximately 40 kDa (Figure 4.4 A). The samples under non-reducing conditions showed a higher band on gel, indicating the presence of a homodimeric protein complex. The exact size of the higher bands cannot be determined in this experiment, as bands resulting from non-reduced proteins cannot be compared with the used marker. However, with size exclusion chromatography (SEC), a mass of approximately 83,900 Da was determined, which is in concordance with the theoretical size of a VHH-pa2H-Fc homodimer (Figure 4.4 B).

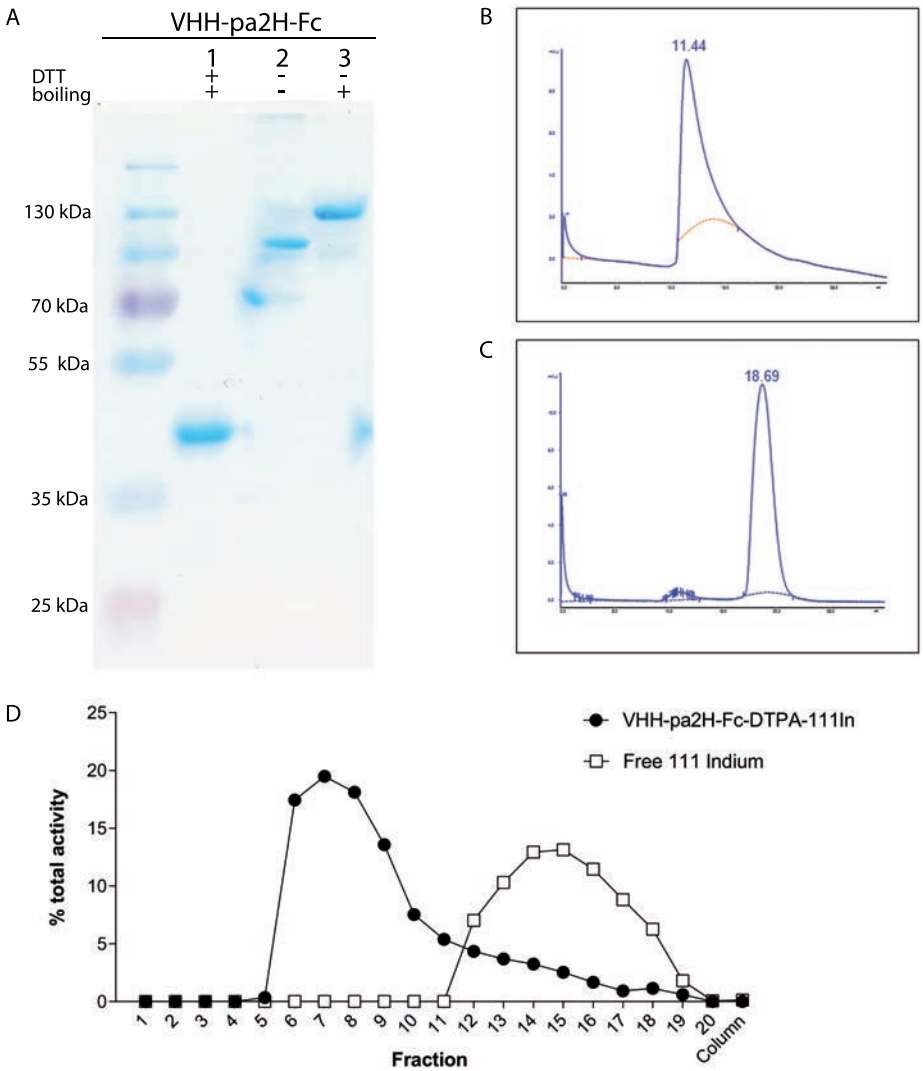

Figure 4.4. Quality control of VHH-pa2H-Fc, VHH-pa2H-Fc-DTPA and VHH-pa2H-Fc-DTPA-^{111}In. **(A)** SDS-PAGE analysis of VHH-pa2H-Fc under denaturing (+DTT) and non-denaturing (-DTT) conditions shows a denatured protein at approximately 42 kDa and much higher bands under non-denaturing conditions, indicating the formation of a complex protein. **(B + C)** Size exclusion chromatography confirms the addition of at least one DTPA molecule to VHH-pa2H-Fc as indicated by the near-complete shift of the peak from 11.44 to 18.69 ml. **(D)** PD-10 column purification indicated highly successful radiolabeling of ^{111}In to the DTPA labeled VHH-pa2H-Fc, as no significant peaks were detected in fractions 12-18, in which free radiotracer elutes from the column.

3.3. DTPA conjugation to VHH-pa2H-Fc and radiolabeling with ^{111}In

Successful DTPA conjugation to the fusion protein was confirmed with SEC, in which the retention time of the peak for the non-radiolabeled VHH-pa2H-Fc almost completely shifted from 11.44 to 18.69 ml after the conjugation (Figure 4.4 B and C). After radiolabeling, VHH-pa2H-Fc-DTPA-^{111}In was purified on a PD-10 column to remove labelling reactants. The highest radioac-

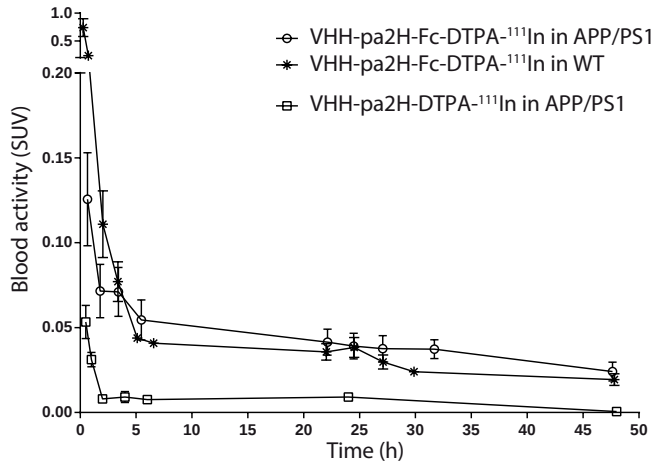

Figure 4.5. Pharmacokinetics. Blood clearance of VHH-pa2H-DTPA-^{111}In and VHH-pa2H-Fc-DTPA-^{111}In in double transgenic APP$_{swe}$/PS1dE9 (APP/PS1) and wildtype littermates (WT). Data are mean ± SEM of 4-8 observations at time points up to 48 h after injection and are shown as standard uptake values (SUV).

Table 4.1. Area Under the Curve (AUC) values calculated based on the data depicted in Figure 4.5, show significant increases for the Fc fused VHH compared to the non-fused VHH-pa2H in APP$_{swe}$/PS1dE9 transgenic mice (APP/PS1) and wildtype littermates (WT). All mice were injected with 20 μg VHH labeled with ^{111}In at 10-20 MBq at the time of injection.

	VHH-pa2H-DTPA-^{111}In		VHH-pa2H-Fc-DTPA-^{111}In	
	WT	**APP/PS1**	**WT**	**APP/PS1**
n	-	4	8	8
AUC	nd	17.1 ± 2.7	116.3 ± 12.3 *	124.7 ± 21.3 *

*=p<0.05 compared to VHH-pa2H-DTPA-^{111}In, nd = not determined.

tivity was found in fractions 6-9 (Figure 4.4 D), which were pooled for *in vivo* administration. No significant peaks were detected in the shoulder in fractions 12-18, indicating the absence of free ^{111}In. The amount of radioactivity in the pooled fractions amounted to 89% of the total radioactivity.

3.4. Pharmacokinetics

The blood clearance of the VHH fusion protein VHH-pa2H-Fc-DTPA-^{111}In and the control tracer VHH-pa2H-DTPA-^{111}In were calculated and expressed as SUV, from which the AUC was calculated (Figure 4.5 and Table 4.1). Based on the AUC values and clearance graphs it is clear that the fusion of the human IgG Fc domain leads to a significant increase in retention in the blood of the fused VHH compared to the unmodified VHH-pa2H. Even though slightly higher in the transgenic group, between the APP/PS1 group and the WT littermates the AUC of the blood clearance of VHH-pa2H-Fc-DTPA-^{111}In was not significantly different.

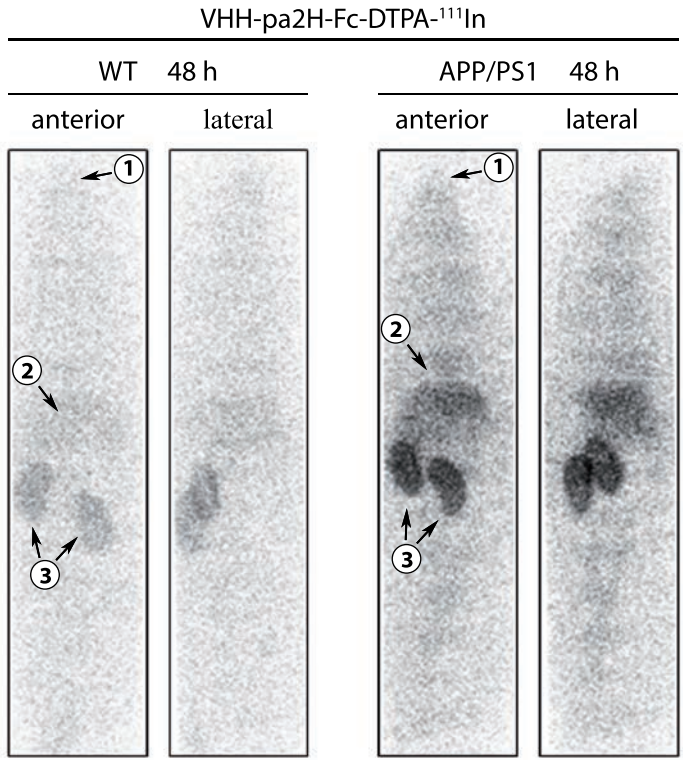

Figure 4.6. Anterior and lateral microSPECT scintigraphs show the difference in biodistribution and pharmacokinetic profile of VHH-pa2H-Fc-DTPA-^{111}In between double transgenic APP$_{swe}$/PS1dE9 (APP/PS1) and wildtype littermates (WT) at 48 h after injection. In both strains, the majority of the signal originates from the kidneys (3) and the liver (2), while the brain (1) does not contain more signal compared to the rest of the body. Overall, there seems to be less signal originating from the WT animals compared to the APP/PS1, which is in concordance with the data obtained from the pharmacokinetics. All mice were injected with 20 µg VHH labeled with ^{111}In at 10-20 MBq at the time of injection and imaged at 48 h for 30 minutes.

3.5. MicroSPECT imaging

MicroSPECT imaging of the mice injected with VHH-pa2H-Fc-DTPA-^{111}In confirmed that the Fc-fused VHH was still present in the mice at 48 h, mainly in the renal cortex and in the liver (Figure 4.6). However, the images depicted clearly that the protein was not found to be accumulating in the transgenic brains, i.e. at the amyloid deposits, as there was no significant difference in signal in that area between APP/PS1 and WT animals.

3.6. Biodistribution

Radioactivity counts of excised organs and tissues at 48 h after injection showed that the profiles of the Fc tagged VHH generally follow the plasma pharmacokinetics, i.e. higher counts are found in the organs for the VHH-pa2H-Fc-DTPA-^{111}In injected group compared the group injected with the non-Fc VHH (Table 4.2). The kidneys are the main organ of clearance of the radioactivity of VHH-pa2H-Fc-DTPA-^{111}In, corroborating the microSPECT data. For the non-fused

Table 4.2. Biodistribution of VHH-pa2H-DTPA-^{111}In and VHH-pa2H-Fc-DTPA-^{111}In in 12-14 month old double transgenic APP$_{swe}$/PS1dE9 (APP/PS1) and wildtype littermates (WT) at 48 h after injection. Values are presented as the mean ± SEM of the radioactivity counted per weighed tissue after sacrificing and corrected for total body weight expressed as the standard uptake value (SUV) of 4-8 observations. All values are corrected for radioactive decay over time, nd = not determined. All mice were injected with 20 µg VHH labeled with ^{111}In at 10-20 MBq at the time of injection and blood and all tissues were obtained at approximately 48 h after injection.

	VHH-pa2H-DTPA-^{111}In		VHH-pa2H-Fc-DTPA-^{111}In	
	WT	APP/PS1	WT	APP/PS1
n	-	4	8	8
	SUV ± SEM (*SUV = %ID / g tissue per g mouse*)			
Blood	nd	0.0007 ± 0.0001	0.0194 ± 0.0034 *	0.0242 ± 0.0149 *¶
Urine & bladder	nd	0.0291 ± 00079	0.0237 ± 0.0036	0.0140 ± 0.0025
Heart	nd	0.0015 ± 0.0003	0.0099 ± 0.0011 *	0.0121 ± 0.0022 *¶
Lungs	nd	0.0016 ± 0.0002	0.0188 ± 0.0018 *	0.0188 ± 0.0035 *¶
Spleen	nd	0.2939 ± 0.1362	0.0412 ± 0.0072 *	0.0207 ± 0.0037 *¶
Liver	nd	0.0007 ± 0.0001	0.0658 ± 0.0108 *	0.0135 ± 0.0091
Kidneys	nd	0.1493 ± 0.0095	0.2194 ± 0.0119 *	0.0874 ± 0.0455
Muscle	nd	0.0008 ± 0.0001	0.0054 ± 0.0012	0.0048 ± 0.0009 *¶
Cerebrum	nd	0.0001 ± 0.0000	0.0011 ± 0.0004	0.0008 ± 0.0003
Cerebellum	nd	0.0003 ± 0.0003	0.007 ± 0.0001 *	0.0008 ± 0.0002 *
Brain	nd	0.0004 ± 0.0002	0.0017 ± 0.0005	0.0016 ± 0.0005
Brain/blood ratio	nd	0.5796 ± 0.1546	0.0829 ± 0.0059 *	0.0640 ± 0.0066 *¶
Muscle/blood ratio	nd	1.3040 ± 0.4035	0.3192 ± 0.0761 *	0.2225 ± 0.0219 *¶
Ratio brain/blood to muscle/blood	nd	0.4376 ± 0.1083	0.3719 ± 0.1041	0.3157 ± 0.0629

* = $p < 0.05$ compared to VHH-pa2H-DTPA-^{111}In; ¶ = $p < 0.05$ compared to WT mice.

VHH, 98.10 ± 0.04 %ID is secreted after 48 h, with the remainder residing mainly in the spleen. This secretion is significantly higher ($p<0.006$) compared to the fusion protein VHH-pa2H-Fc-DTPA-^{111}In in both the transgenic mice (92.47 ± 0.59 %ID) and the WT littermates (94.77 ± 0.19 %ID) at 48 h after injection. For VHH-pa2H-Fc-DTPA-^{111}In the excretion was significantly lower ($p<0.01$) in APP/PS1 mice compared to WT animals.

When analyzing the amount of radioactivity found in the brain, it is interesting to note that the brain to blood ratio seems to be significantly higher for the non-fused VHH than for the Fc fused moieties. However, by comparing this ratio to the muscle to blood ratio, a calculation which indicates the specificity of the brain to blood ratio, it is clear that the exceedingly low blood values in the non Fc fused VHH group are confounding the obtained ratios. The ratio "brain/blood to muscle/blood" is not significantly different between any of the analyzed groups.

4. DISCUSSION

In this study we provide evidence that the blood clearance of VHH-pa2H-DTPA-^{111}In in WT and APP/PS1 transgenic mice can be significantly slowed down by fusion to the Fc region of the human IgG protein. Earlier we have shown that free, unmodified VHH have a fast blood clearance profile and may not effectively cross the *in vivo* BBB; a limitation which must be overcome for the development of brain amyloid targeted diagnostics or therapeutics in AD [8,10]. The rapid renal clearance of non-Fc tagged VHH-pa2H-DTPA-^{111}In is once more confirmed in this study (Figure 4.5 and Table 4.2).

As the transport of these Aβ-targeting VHH over the BBB is an active process [30,34,35], we hypothesized that prolonging the blood residential time of the VHH could increase its delivery into the brain. To achieve this, a human IgG1 Fc domain (hinge, CH_2 and CH_3 region) was fused to the C-terminus of VHH-pa2H (Figure 4.1). As a result, the homodimer forming fusion protein reached a total molecular weight of 80 kDa, above the renal filtration cut-off of approximately 60 kDa. Furthermore, interaction of the fusion protein with the FcRn provides additional systemic retention of the construct. As the increased AUC values show, the fusion of the Fc domain did indeed significantly prolong the blood residential time of the VHH-pa2H-Fc-DTPA-^{111}In (Figure 4.5).

Between the two groups of mice – the APP/PS1 double transgenic and the WT littermates – there is no significant difference in retention of VHH-pa2H-Fc-DTPA-^{111}In. This indicates that indeed the presence of the Fc tail, rather than the presence of an Aβ phenotype, is the cause of the increased retention in the circulation, even if the trend in the AUC graph and values indicates a slightly higher retention in the APP/PS1 animals (Figure 4.5). This trend is also observed

in the microSPECT images obtained at 48 h after injection, in which certain organs, most notably the kidneys and the liver, seem to have a slightly stronger signal (Figure 4.6). In accordance, less radioactivity was excreted from transgenic mice compared to WT at 48 h.

The pharmacokinetics data (Figure 4.5) furthermore suggest a dramatic reduction in volume of distribution (VD) as a result of the fusion of the Fc tail. This is especially pronounced in the WT group injected with VHH-pa2H-Fc-DTPA-^{111}In. This would indicate that the unmodified VHH-pa2H-DTPA-^{111}In is more rapidly distributed over the organs and tissues in the animal body, while the Fc-fused protein remains in the bloodstream. However, keeping in mind that unmodified VHH have significantly shorter blood half-lives and are quickly cleared by the renal system, it must be noted that the organ biodistribution profile should be analyzed shortly after injection to confidently calculate actual VD values.

The biodistribution data (Table 4.2) show that most organs in the groups injected with VHH-pa2H-Fc-DTPA-^{111}In have significantly higher SUVs compared to the non-fused VHH. However, when the ratios between the brain-to-blood and muscle-to-blood are compared, it is clear that there is no relative increase in uptake in the brain compared to uptake in the muscle. Interestingly, there is no specific increase in the brain of the transgenic animals compared to the WT littermates either. In previous studies, it has been shown that once the VHH reaches the amyloid deposits in the brain, the antibody fragments remains associated with the amyloid and will this be retained in the brain [8,10]. It can therefore be assumed that VHH-pa2H-Fc-DTPA-^{111}In does not reach the BBB protected brain more efficiently than the non-fused VHH-pa2H-DTPA-^{111}In, despite the increased blood circulation time.

The 80 kDa size of the VHH-Fc, a significant increase over the 12 kDa of the unmodified VHH, may hypothetically obstruct the blood-brain barrier passage. However, an increase in size of the VHH does not necessarily exclude BBB passage [9]. Even full length IgGs can be transported over the BBB when an active transport is involved [36,37], as is the case with the VHHs. Indeed, Farrington *et al.* recently described the enhanced *in vivo* passage of an Fc tagged VHH compared to the free VHH over the rat BBB [27]. It must be noted however, that in the latter example a 5-15 times higher concentration of VHH-fc derivative had been injected compared to the current study and species differences might play a role in the amount of BBB penetration [38].

The VHH-pa2H-Fc construct does, however, recognize Aβ (Figure 4.3). Fusion of the Fc region to the antibody fragment is therefore not detrimental to its function, and may in fact improve its binding capacity [27]. As a result, VHH-pa2H-Fc could still be used for peripheral applications in general and more specifically investigated for use in the peripheral sink theory [39–41]. Furthermore, it also means that the concept of VHH-Fc fusion proteins can be extrapolated to other VHHs. In this study we did not examine whether the VHH-pa2H-Fc-DTPA-^{111}In in the

blood is free in the plasma or bound to circulating host cells. It may be plausible that the interaction of the fusion protein with Fc receptors or other compounds increases the blood residential time, but also actively prevents the fusion protein to reach and cross the BBB [42].

The use of the chelator p-SCN-Bz-DTPA to label VHH-pa2H and VHH-pa2H-Fc with ^{111}In could cause the VHH to act differently in an *in vivo* setting. However, based on the experiments in this study (Figure 4.3) and on previous experience, we know that the DTPA labeling has no effect on the amyloid beta binding characteristics of the VHH [8,10], and that the labeling itself is very stable over time [8]. Also, it has been shown that conjugation with Alexa dyes, which occurs via a similar NHS-ester conjugation, shows no difference in characteristic binding or biodistribution profiles for single VHHs [10], or for Fc conjugated VHHs [27] and that the similar binding of a NOTA chelator can be used to follow the biodistribution of VHHs *in vivo* [43].

5. CONCLUSION

VHH-pa2H-Fc can be effectively produced in HEK293T cells and retains its biological activity. It shows significantly increased systemic retention due to the fusion of the llama antibody fragment to the hinge, CH_2 and CH_3 domains of a human IgG1. However, increasing the blood circulation time alone does not result in increased BBB penetration.

DISCLOSURE

No potential conflicts of interest are to be disclosed.

ACKNOWLEDGMENTS

The authors wish to acknowledge Ernst Suidgeest and Tessa Buckle (Leiden University Medical Center, NL) for their technical assistance and Hendrik Adams (BAC b.v., NL) for supplying the VHH-pa2H. This research was performed within the framework project LeARN (grant 02N-101) and the Center for Medical Systems Biology (grants S-MRI-110010 and S-MRI-110030).

REFERENCES

1. Yardehnavi, N., Behdani, M., Pooshang Bagheri, K., Mahmoodzadeh, A., Khanahmad, H., Shahbazzadeh, D., Habibi-Anbouhi, M., Ghassabeh, G. H. & Muyldermans, S. A camelid antibody candidate for development of a therapeutic agent against Hemiscorpius lepturus envenomation. *FASEB J.* 28(9):4004–14 (2014).
2. Hmila, I., Abdallah R, B. A. Ben, Saerens, D., Benlasfar, Z., Conrath, K., Ayeb, M. El, Muyldermans, S. & Bouhaouala-Zahar, B. VHH, bivalent domains and chimeric Heavy chain-only antibodies with high neutralizing efficacy for scorpion toxin AahI'. *Mol. Immunol.* 45(14):3847–3856 (2008).
3. Gad, W., Ben-Abderrazek, R., Wahni, K., Vertommen, D., Muyldermans, S., Bouhaouala-Zahar, B. & Messens, J. Wheat germ in vitro translation to produce one of the most toxic sodium channel specific toxins. *Biosci. Rep.* 34(4) (2014).
4. Cardoso, F. M., Ibañez, L. I., Van den Hoecke, S., De Baets, S., Smet, A., Roose, K., Schepens, B., Descamps, F. J., Fiers, W., Muyldermans, S., *et al.* Single-domain antibodies targeting neuraminidase protect against an H5N1 influenza virus challenge. *J. Virol.* 88(15):8278–96 (2014).
5. Scheuplein, F., Rissiek, B., Driver, J. P., Chen, Y.-G., Koch-Nolte, F. & Serreze, D. V. A recombinant heavy chain antibody approach blocks ART2 mediated deletion of an iNKT cell population that upon activation inhibits autoimmune diabetes. *J. Autoimmun.* 34(2):145–54 (2010).
6. Impagliazzo, A., Tepper, A. W., Verrips, T. C., Ubbink, M. & van der Maarel, S. M. Structural basis for a PABPN1 aggregation-preventing antibody fragment in OPMD. *FEBS Lett.* 584(8):1558–64 (2010).
7. Rutgers, K. S., van Remoortere, A., van Buchem, M. A., Verrips, C. T., Greenberg, S. M., Bacskai, B. J., Frosch, M. P., van Duinen, S. G., Maat-Schieman, M. L. & Van der Maarel, S. M. Differential recognition of vascular and parenchymal beta amyloid deposition. *Neurobiol. Aging* 32(10):1774–1783 (2009).
8. Rotman, M., Welling, M. M., Bunschoten, A., de Backer, M. E., Rip, J., Nabuurs, R. J. A., Gaillard, P. J., van Buchem, M., van der Maarel, S. M. & van der Weerd, L. Enhanced liposomal brain delivery of an anti-amyloid VHH-2H heavy chain antibody fragment in a mouse model for Alzheimer's disease. *J. Control. Release* 203:40–50 (2015).
9. Li, T., Bourgeois, J.-P., Celli, S., Glacial, F., Le Sourd, A.-M., Mecheri, S., Weksler, B., Romero, I., Couraud, P.-O., Rougeon, F., *et al.* Cell-penetrating anti-GFAP VHH and corresponding fluorescent fusion protein VHH-GFP spontaneously cross the blood-brain barrier and specifically recognize astrocytes: application to brain imaging. *FASEB J.* 26(10):3969–79 (2012).
10. Nabuurs, R. J. A., Rutgers, K. S., Welling, M. M., Metaxas, A., de Backer, M. E., Rotman, M., Bacskai, B. J., van Buchem, M. A., van der Maarel, S. M. & van der Weerd, L. *In vivo* detection of amyloid-β deposits using heavy chain antibody fragments in a transgenic mouse model for Alzheimer's disease. *PLoS One* 7(6):e38284 (2012).
11. Rotman, M., Snoeks, T. J. A. & van der Weerd, L. Pre-clinical optical imaging and MRI for drug development in Alzheimer's disease. *Drug Discovery Today: Technologies* 8(2-4):e117–e125 (2011).
12. Kontermann, R. E. Strategies to extend plasma half-lives of recombinant antibodies. *BioDrugs* 23(2):93–109 (2009).
13. Kontermann, R. E. Strategies for extended serum half-life of protein therapeutics. *Curr. Opin. Biotechnol.* 22(6):868–76 (2011).
14. Gunasekaran, K., Pentony, M., Shen, M., Garrett, L., Forte, C., Woodward, A., Ng, S. Bin, Born, T., Retter, M., Manchulenko, K., *et al.* Enhancing antibody Fc heterodimer formation through electrostatic steering effects: applications to bispecific molecules and monovalent IgG. *J. Biol. Chem.* 285(25):19637–46 (2010).
15. Martin, W. L., West, A. P., Gan, L. & Bjorkman, P. J. Crystal structure at 2.8 A of an FcRn/heterodimeric Fc complex: mechanism of pH-dependent binding. *Mol. Cell* 7(4):867–77 (2001).

16. Olafsen, T., Kenanova, V. E. & Wu, A. M. Tunable pharmacokinetics: modifying the *in vivo* half-life of antibodies by directed mutagenesis of the Fc fragment. *Nat. Protoc.* 1(4):2048–60 (2006).

17. Ying, T., Ju, T. W., Wang, Y., Prabakaran, P. & Dimitrov, D. S. Interactions of IgG1 CH_2 and CH_3 Domains with FcRn. *Front. Immunol.* 5:146 (2014).

18. Gould, L. H., Sui, J., Foellmer, H., Oliphant, T., Wang, T., Ledizet, M., Murakami, A., Noonan, K., Lambeth, C., Kar, K., *et al.* Protective and therapeutic capacity of human single-chain Fv-Fc fusion proteins against West Nile virus. *J. Virol.* 79(23):14606–13 (2005).

19. Ono, K.-I., Kamihira, M., Kuga, Y., Matsumoto, H., Hotta, A., Itoh, T., Nishijima, K.-I., Nakamura, N., Matsuda, H. & Iijima, S. Production of anti-prion scFv-Fc fusion proteins by recombinant animal cells. *J. Biosci. Bioeng.* 95(3):231–8 (2003).

20. Kamihira, M., Ono, K., Esaka, K., Nishijima, K., Kigaku, R., Komatsu, H., Yamashita, T., Kyogoku, K. & Iijima, S. High-level expression of single-chain Fv-Fc fusion protein in serum and egg white of genetically manipulated chickens by using a retroviral vector. *J. Virol.* 79(17):10864–74 (2005).

21. Powers, D. B., Amersdorfer, P., Poul, M., Nielsen, U. B., Shalaby, M. R., Adams, G. P., Weiner, L. M. & Marks, J. D. Expression of single-chain Fv-Fc fusions in Pichia pastoris. *J. Immunol. Methods* 251(1-2):123–35 (2001).

22. Richard, G., Meyers, A. J., McLean, M. D., Arbabi-Ghahroudi, M., MacKenzie, R. & Hall, J. C. *In vivo* neutralization of α-cobratoxin with high-affinity llama single-domain antibodies (VHHs) and a VHH-Fc antibody. *PLoS One* 8(7):e69495 (2013).

23. De Buck, S., Virdi, V., De Meyer, T., De Wilde, K., Piron, R., Nolf, J., Van Lerberge, E., De Paepe, A. & Depicker, A. Production of camel-like antibodies in plants. *Methods Mol. Biol.* 911:305–24 (2012).

24. De Buck, S., Nolf, J., De Meyer, T., Virdi, V., De Wilde, K., Van Lerberge, E., Van Droogenbroeck, B. & Depicker, A. Fusion of an Fc chain to a VHH boosts the accumulation levels in Arabidopsis seeds. *Plant Biotechnol. J.* 11(8):1006–16 (2013).

25. Veggiani, G., Ossolengo, G., Aliprandi, M., Cavallaro, U. & de Marco, A. Single-domain antibodies that compete with the natural ligand fibroblast growth factor block the internalization of the fibroblast growth factor receptor 1. *Biochem. Biophys. Res. Commun.* 408(4):692–6 (2011).

26. Bell, A., Wang, Z. J., Arbabi-Ghahroudi, M., Chang, T. a, Durocher, Y., Trojahn, U., Baardsnes, J., Jaramillo, M. L., Li, S., Baral, T. N., *et al.* Differential tumor-targeting abilities of three single-domain antibody formats. *Cancer Lett.* 289(1):81–90 (2010).

27. Farrington, G. K., Caram-Salas, N., Haqqani, A. S., Brunette, E., Eldredge, J., Pepinsky, B., Antognetti, G., Baumann, E., Ding, W., Garber, E., *et al.* A novel platform for engineering blood-brain barrier-crossing bispecific biologics. *FASEB J.* 28(11):4764–4778 (2014).

28. Bazl, M. R., Rasaee, M. J., Foruzandeh, M., Rahimpour, A., Kiani, J., Rahbarizadeh, F., Alirezapour, B. & Mohammadi, M. Production of chimeric recombinant single domain antibody-green fluorescent fusion protein in Chinese hamster ovary cells. *Hybridoma* (*Larchmt*). 26(1):1–9 (2007).

29. Aliprandi, M., Sparacio, E., Pivetta, F., Ossolengo, G., Maestro, R. & de Marco, A. The availability of a recombinant anti-SNAP antibody in VHH format amplifies the application flexibility of SNAP-tagged proteins. *J. Biomed. Biotechnol.* 2010:658954 (2010).

30. Rutgers, K. S., Nabuurs, R. J. A., van den Berg, S. A. A., Schenk, G. J., Rotman, M., Verrips, C. T., van Duinen, S. G., Maat-Schieman, M. L., van Buchem, M. A., de Boer, A. G., *et al.* Transmigration of beta amyloid specific heavy chain antibody fragments across the *in vitro* blood-brain barrier. *Neuroscience* 190:37–42 (2011).

31. Reiserer, R. S., Harrison, F. E., Syverud, D. C. & McDonald, M. P. Impaired spatial learning in the APPSwe + PSEN1DeltaE9 bigenic mouse model of Alzheimer's disease. *Genes. Brain. Behav.* 6(1):54–65 (2007).

32. Jankowsky, J. L., Fadale, D. J., Anderson, J., Xu, G. M., Gonzales, V., Jenkins, N. A., Copeland, N. G., Lee, M. K., Younkin, L. H., Wagner, S. L., *et al.* Mutant presenilins specifically elevate the levels of the 42 residue beta-amyloid peptide *in vivo*: evidence for augmentation of a 42-specific gamma secretase. *Hum. Mol. Genet.* 13(2):159–70 (2004).

33. Loening, A. M. & Gambhir, S. S. AMIDE: a free software tool for multimodality medical image analysis. *Mol. Imaging* 2(3):131–7 (2003).

34. Abulrob, A., Sprong, H., Van Bergen en Henegouwen, P. & Stanimirovic, D. The blood-brain barrier transmigrating single domain antibody: mechanisms of transport and antigenic epitopes in human brain endothelial cells. *J. Neurochem.* 95(4):1201–14 (2005).

35. Muruganandam, A., Tanha, J., Narang, S. & Stanimirovic, D. Selection of phage-displayed llama single-domain antibodies that transmigrate across human blood-brain barrier endothelium. *FASEB J.* 16(2):240–2 (2002).

36. Pardridge, W. M. & Boado, R. J. Reengineering biopharmaceuticals for targeted delivery across the blood-brain barrier. *Methods Enzymol.* 503:269–92 (2012).

37. Niewoehner, J., Bohrmann, B., Collin, L., Urich, E., Sade, H., Maier, P., Rueger, P., Stracke, J. O., Lau, W., Tissot, A. C., *et al.* Increased brain penetration and potency of a therapeutic antibody using a monovalent molecular shuttle. *Neuron* 81(1):49–60 (2014).

38. Warren, M. S., Zerangue, N., Woodford, K., Roberts, L. M., Tate, E. H., Feng, B., Li, C., Feuerstein, T. J., Gibbs, J., Smith, B., *et al.* Comparative gene expression profiles of ABC transporters in brain microvessel endothelial cells and brain in five species including human. *Pharmacol. Res.* 59(6):404–13 (2009).

39. Wang, Y.-J., Gao, C.-Y., Yang, M., Liu, X.-H., Sun, Y., Pollard, A., Dong, X.-Y., Wu, X.-B., Zhong, J.-H., Zhou, H.-D., *et al.* Intramuscular delivery of a single chain antibody gene prevents brain Aβ deposition and cognitive impairment in a mouse model of Alzheimer's disease. *Brain. Behav. Immun.* 24(8):1281–93 (2010).

40. Sagare, A., Deane, R., Bell, R. D., Johnson, B., Hamm, K., Pendu, R., Marky, A., Lenting, P. J., Wu, Z., Zarcone, T., *et al.* Clearance of amyloid-beta by circulating lipoprotein receptors. *Nat. Med.* 13(9):1029–31 (2007).

41. Weiner, H. L. & Frenkel, D. Immunology and immunotherapy of Alzheimer's disease. *Nat. Rev. Immunol.* 6(5):404–16 (2006).

42. Tarzi, R. M., Davies, K. A., Robson, M. G., Fossati-Jimack, L., Saito, T., Walport, M. J. & Cook, H. T. Nephrotoxic nephritis is mediated by Fcγ receptors on circulating leukocytes and not intrinsic renal cells. *Kidney Int.* 62(6):2087–2096 (2002).

43. Morais, M., Cantante, C., Gano, L., Santos, I., Lourenço, S., Santos, C., Fontes, C., Aires da Silva, F., Gonçalves, J. & Correia, J. D. G. Biodistribution of a (67)Ga-labeled anti-TNF VHH single-domain antibody containing a bacterial albumin-binding domain (Zag). *Nucl. Med. Biol.* 41 Suppl:e44–8 (2014).

1. Department of Human Genetics, Leiden University Medical Center, The Netherlands
2. Department of Radiology, Leiden University Medical Center, The Netherlands
3. Department of Neuroscience, Mayo Clinic, Jacksonville, FL, USA